International Journal of Automotive Technology, Vol. 8, No. 3, pp. 383–394 (2007)

1229–9138/2007/034–15

ENHANCED FUZZY SLIDING MODE CONTROLLER FOR LAUNCH CONTROL OF AMT VEHICLE USING A BRUSHLESS DC MOTOR DRIVE

Y.-S. ZHAO[1,2], L.-P. CHEN[1], Y.-Q. ZHANG[1] and J. YANG[3]*

[1]Center for Computer-Aided Design, School of Mechanical Science & Engineering, Huazhong University of Science & Technology, Wuhan, Hubei 430074, China
[2]Center for CAD/CAM, School of Mechanical Engineering & Applied Electronics Technology, Beijing University of Technology, Beijing 100022, China
[3]Center for Computer-Aided Design, The University of Iowa, 111 Engineering Research Facility, Iowa City, IA 52246, USA

(Received 12 July 2006/Revised 21 November 2006)

ABSTRACT–Due to the clutch's non-linear dynamics, time-delays, external disturbance and parameter uncertainty, the automated clutch is difficult to control precisely during the launch process for automatic mechanical transmission (AMT) vehicles. In this paper, an enhanced fuzzy sliding mode controller (EFSMC) is proposed to control the automated clutch. The sliding and global stability conditions are formulated and analyzed in terms of the Lyapunov full quadratic form. The chattering phenomenon is handled by using a saturation function to replace the pure sign function and fuzzy logic adaptation system in the control law. To meet the real-time requirement of the automated clutch, the region-wise linear technology is adopted to reduce the fuzzy rules of the EFSMC. The simulation results have shown that the proposed controller can achieve a higher performance with minimum reaching time and smooth control actions. In addition, our data also show that the controller is effective and robust to the parametric variation and external disturbance.

KEY WORDS : AMT, Automated clutch, Brushless DC motor, Sliding mode control, Fuzzy control

NOMENCLATURE

i_{as}, i_{ibs}, i_{cs} : currents of the two-phase stator coils
v_{as}, v_{bs}, v_{cs} : voltages of the two-phase stator coils
J_e : moment of inertia of the rotor
k_T : coefficient of the equivalent torque of resistance
L : resistance and inductance of the three-phase stator coils
M : denotes mutual-inductance of three-phase stator coils
p : number of poles of the rotor
R : resistance and inductance of the three-phase stator coils
V_{DC} : voltage of the DC supplying resource
λ_m : amplitude of the flux-linkage built by the permanent magnet
θ_r : electric angle of the rotor defined as the angle between d-axis and a-phase axis stator
ω_r : angular velocity of the rotor
A_d : peak value of the triangle signal
B_m : damping coefficient of the rotor
c_m : damping coefficient of the membrane spring

*Corresponding author. e-mail: jyang@engineering.uiowa.edu

1. INTRODUCTION

In recent years, the AMT has gained much more attention (Chen *et al.*, 2000; Shen and Wu, 1999; Hahn and Lee, 2002). The system consists of a manual gear shift device with an actuator, and a clutch and a gear controlled by an electronic control unit (ECU). The AMT works with the actuator which a program controls according to the vehicle's driving condition and the driver's intention. When compared with automatic transmission (AT) systems, the AMT offers some advantages in terms of overall system costs (simpler system) and fuel consumption (higher mechanical efficiency). Significant fuel savings of 4~5% on the standard driving cycle are advantageous given market demands (Montanari and Ronchi, 2004).

As an important subsystem of the AMT, the automated clutch can be declutched and engaged automatically. The engagement must be controlled to satisfy different and sometimes conflicting objectives, such as small friction

losses, minimum time needed for the engagement and preservation of driver comfort during the launch process. A proper normal force to the clutch-driven disk is the key to satisfy all of these goals. There are two issues in controlling the clutch properly, one is how to implement the engagement law, and the other is how to make the clutch follow the law in a timely manner (Liu *et al.*, 2002). The controller can be divided into upper level and lower level, where the upper level is used as the engagement law that includes the description and abstraction of the system, the identification of the symbol and environment as well as the controlling law's online studying and adjusting the lower level, mainly discussed in this paper, is used to enforce the clutch to follow the engaging law. But tracking control involving the automated clutch of AMT has several difficulties owing to clutch's non-linear dynamics, time-delays, parameter uncertainty and external disturbance (Gaillard and Singh, 2000).

Several control strategies have been developed for controlling the motion of the automated clutch of AMT driven by electropneumatic (Tanaka and Wada, 1995), electrohydraulic (Horn *et al.*, 2003; Glielmo *et al.*, 2006) or electromechanical approach (Zhang *et al.*, 2002), in which H^{∞} control theory (Hibino *et al.*, 1996), the fuzzy control (Hayashi *et al.*, 1993) and optimal control (David and Natarajan, 2005) are applied, respectively. James and Loh (Slicker and Loh, 1996) have presented the design of a vehicle launch control system for AMT. Zanasi (Zanasi and Visconti, 2001) has discussed dynamic modeling and engagement control for the automotive dry clutch. Garofalo and Glielmo (Garofalo and Glielmo, 2001; Glielmo and Vasca, 2000) have considered the control of the dry clutch engagement process for the automotive application in which the slip control technique and linear quadratic state feedback controller are applied to solve a finite time optimal control problem. These control algorithms have computational efficiency and are easy to implement.

This paper mainly discusses trajectory tracking of the clutch position using a brushless DC motor as the actuator during the launch process. Compared with hydraulic servo systems (Montanari and Ronchi, 2004), the brushless DC motor driving system has several advantages such as higher efficiency and saving space (Lee and Youn, 2004). To obtain the optimum operating control of the automated clutch of AMT, it is necessary to investigate the automated clutch system with an advanced control law. Fuzzy sliding mode control (FSMC) has been applied in control engineering (Ha *et al.*, 1999; Kaynak *et al.*, 2001; Yu *et al.*, 2003) as a robust and precise algorithm. However, an inevitable chattering from the switch of the control structure exists, and this will cause torque ripple. Furthermore, the expensive computing requirement of the complicated algorithm in FSMC may also limit its on-line application to the automated clutch. This paper proposes EFSMC to track the desired trajectory. In order to control the automated clutch in real-time, the region-wise linear technique is adopted to reduce the number of the fuzzy rules for the fuzzy logic adaptive controller. The simulation results will demonstrate the advantages of the enhanced fuzzy sliding mode control system.

The organization of this paper is as follows. In Section 2, the automated clutch system and dynamics analysis are discussed. The conventional sliding mode controller (CSMC) is designed in Section 3. An enhanced fuzzy sliding mode controller is proposed in Section 4. The numerical simulation results are compared for the automated clutch system with CSMC and EFSMC in Section 5. Finally, several conclusions are drawn in Section 6.

2. AUTOMATED CLUTCH SYSTEM AND DYNAMIC ANALYSIS

An accurate system model is the key for the controller design and dynamic analysis of the automated clutch. Although the physically full-order model of the clutch system can be theoretically derived to demonstrate its validity, it is not practically suitable for the controller design due to its complexity. In this paper, the J4001050917016 transmission (Transmission of AUTO., 2005) used in a JNJ7080A vehicle is adopted and a reduced model is therefore derived intentionally for the design of the position controller.

The simplified schematic of the clutch control system is depicted in Figure 1. The clutch consists of two disks connected to the engine shaft and to the gear-box shaft in the driveline. It is possible to control the clutch position using a mechanical actuator that is driven by a brushless DC motor. In this way, the torque transmitted from the engine to the wheels can be modulated and the shift change will be available during the disengagement phase where the clutch system includes two parts: the brushless DC motor and the clutch with the mechanical actuator.

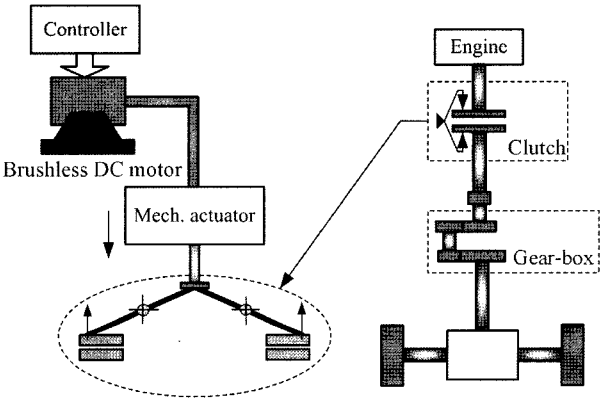

Figure. 1 Automated clutch system scheme.

2.1. Modeling of Brushless DC Motor

Physically, a brushless DC motor has the same structure as a synchronous machine, which has high torque generation with a low speed. In this research, a brushless DC motor is adopted to act as the electronic servo actuator. The sine induction electromotive force may be generated by the motor, and the three coils of the stator are identical and distributed equally around at an angle of 120 degrees. Thus, the voltage equations of the coils of the stator can be written in a matrix form as follows (Chen and Tang, 1999; Wu *et al.*, 2005).

$$\begin{bmatrix} v_{as} \\ v_{bs} \\ v_{cs} \end{bmatrix} = \begin{bmatrix} R & 0 & 0 \\ 0 & R & 0 \\ 0 & 0 & R \end{bmatrix} \begin{bmatrix} i_{as} \\ i_{bs} \\ i_{cs} \end{bmatrix} + \begin{bmatrix} L-M & 0 & 0 \\ 0 & L-M & 0 \\ 0 & 0 & L-M \end{bmatrix} \frac{d}{dt} \begin{bmatrix} i_{as} \\ i_{bs} \\ i_{cs} \end{bmatrix} + \omega_r \lambda_m \begin{bmatrix} \sin(\theta_r) \\ \sin(\theta_r - 2\pi/3) \\ \sin(\theta_r + 2\pi/3) \end{bmatrix} \tag{1}$$

The dynamic voltage equation of equilibrium for the brushless DC motor with an external torque can be expressed in terms of the rotor angular velocity (Faiz *et al.*, 1996).

$$J_e \left(\frac{2}{p}\right) \frac{d\omega_r}{dt} = T_e - B_m \left(\frac{2}{p}\right) \omega_r - T_L \tag{2}$$

where T_L is the resistant torque of the rotor. T_e is the electromagnetism torque of the motor and can be defined by

$$T_e = \frac{p}{2} \lambda_m [i_{as} \sin\theta_r + i_{bs} \sin(\theta_r - 2\pi/3) + i_{cs} \sin(\theta_r + 2\pi/3)] \tag{3}$$

The general brushless DC motor driving system mainly consists of seven different parts: a brushless DC motor coupled with an actuator, a ramp comparison, a current-controlled PWM voltage source inverter (VSI), a unit vector, a coordinate translator, a current control loop and a clutch position control loop. The brushless DC motor used in this drive system is a three-phase four pole 79.2W, 12V, 5A type.

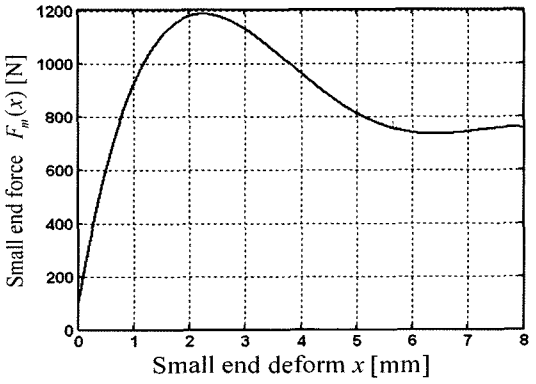

Figure 2. Load-deflection curve for the membrane spring clutch.

2.2. The Dynamic Model of Clutch with the Mechanical Actuator

The lever of the clutch acts as a proportion of force/torque. The equivalent load torque T_L of the motor's rotor relates to the membrane spring force and the displacement x, as

$$T_L = k_T [F_m(x) - c_m \dot{x}] \tag{4}$$

where $F_m(x)$ is the approximate expression of the membrane mechanical performance.

The load-deflection curve for the membrane spring of the clutch is plotted in Figure 2, which was obtained from the experiment data. During numerical applications this nonlinear function can be approximated by a 4th order polynomial in terms of x displacement as

$$F_m(x) = -2.71x^4 + 59.5x^3 - 444.4x^2 + 1218.4x + 87.5 \tag{5}$$

2.3. Simplified Model and State Variable Representation

In the PWM circuit of the brushless DC motor, if the phase's circuit signal $V_1 = A_n \sin(\omega t)$, then the phase voltage v_{as} in equation (1) can be written approximately as

$$v_{as} = \frac{V_{DC} A_m}{2A_d} \sin(\omega t) \tag{6}$$

where A_d denotes the peak value of the triangle signal,

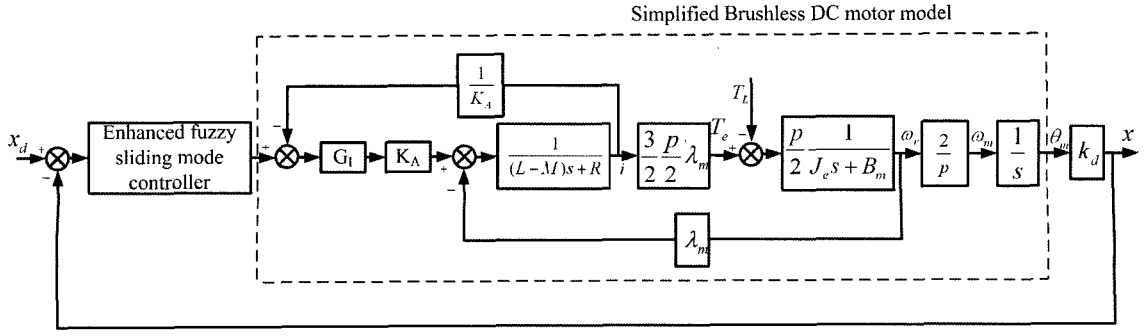

Figure 3. Block diagram of the automated clutch using fuzzy sliding mode controller.

which generates the PWM signal by comparing with V_1. A constant gain for the simplified model of the PWM circuit can be defined as

$$K_A = \frac{v_{as}}{V_1} = \frac{V_{DC}}{2A_d} \tag{7}$$

The decoupling-control technique (Phakamach *et al.*, 2002; Lin *et al.*, 2001) is introduced in this paper; the equation (1), (2) and (7) is transformed by the Laplace transform. Thus, the circuit loop can be simplified to be a single-input-single output system, as shown in Figure 3. The current compensator G_I is used to follow the desired current quickly and efficiently.

If the state variable vector is expressed as $X=[x,\dot{x},\ddot{x}]^T=[x_1,x_2,x_3]^T$, then the mathematic model of the system can be written in the form of a state space

$$\dot{X} = F(X) + GU(t) + f_L I \tag{8}$$

where

$$F(X)=\begin{bmatrix}0 & 1 & 0\\ 0 & 0 & 1\\ 0 & -a_2 & -a_3\end{bmatrix}\begin{bmatrix}x_1\\ x_2\\ x_3\end{bmatrix},\ G=\begin{bmatrix}0\\ 0\\ b\end{bmatrix},\ U(t)=i_q^*,\ I=\begin{bmatrix}0\\ 0\\ 1\end{bmatrix}. \tag{8a}$$

$$a_2 = \frac{8B_m(R+G_I)+3p^2\lambda_m^2}{8J_e(L-M)},\ a_3 = \frac{B_m}{J_e}+\frac{G_I+R}{L-M}, \tag{8b}$$

$$b = \frac{3p\lambda_m k_d G_I k_A}{4J_e(L-M)},\ f_L = -\frac{k_d}{J_e}\dot{T}_L - \frac{k_d(R+G_I)T_L}{J_e(L-M)}. \tag{8c}$$

3. DESIGN OF THE CSMC

This section is a brief review of sliding mode control system. For the automated clutch driven by a brushless DC motor to have a desired error dynamics with a zero steady state error in equation (8), we consider the non-linear, single-input, single-output (SISO) motor-mechanism coupled system

$$\dddot{x}_1(t) = f(X,t) + g(X,t)U(t) + f_L(X,t) \tag{9}$$

where $U(t)$ is the control input vector i_q^*, $f(X,t)$, $g(X,t)$ and $f_L(X,t)$ are approximated by using the estimated functions $\hat{f}(X,t)=-a_2x_2-a_3x_3$, $\hat{g}(X,t)=b$ and

$\hat{f}_L = -\frac{k_d}{J}\dot{T}_L - \frac{k_d(R+G_I)T_L}{J(L-M)}$ respectively, and bounded by known functions $\tilde{f}(X,t)$, $\tilde{g}(X,t)$ and $\tilde{f}_L(X,t)$ obtained by experiment. Therefore, we can rewrite these functions as follows:

$$f(X,t) = \hat{f}(X,t) + \tilde{f}(X,t) \tag{10a}$$

$$g(X,t) = \hat{g}(X,t) + \tilde{g}(X,t) \tag{10b}$$

$$f_L(X,t) = \hat{f}_L(X,t) + \tilde{f}_L(X,t) \tag{10c}$$

The control problem will be to find a control law so that the state X can track the desired trajectories X_d in the presence of the uncertainties. That means that it is required to drive the tracking error asymptotically to zero for any arbitrary initial conditions and uncertainties. Supposing the tracking error vector has the following form

$$E = X - X_d = [e,\ \dot{e},\ \ddot{e}]^T = [e_1,e_2,e_3]^T \tag{11}$$

where

$$X_d = [x_d,\ \dot{x}_d,\ \ddot{x}_d]^T \tag{12}$$

A sliding surface $s(t)$ in the state space R^3 is defined by the scalar function

$$s(X,t)=C_1e_1+C_2e_2+e_3=0 \tag{13}$$

where C_1 and C_2 are constants of sliding mode. The convergence rate of the sliding trajectory depends on the coefficients C_1 and C_2. These coefficients are determined by the Hurwitz condition and pole assignment such that $\dot{s}(X,t)$ has the exponential stability of the sliding dynamics.

The tracking problem will be to find a control law $U(t)$ so that the state X remains on the surface $s(X,t)=0$ for all $t \geq 0$. The control law $U(t)$ consists of the equivalent sliding component $U_{eq}(t)$, which forces the system state to slide on the sliding surface, and the hitting control $U_n(t)$ that drives the states toward the sliding surface. The control law can be chosen from (Yu *et al.*, 1998):

$$U=U_{eq}+U_n \tag{14}$$

3.1. Sliding Mode Control Law Design

From Equation (14), the first step is to determine the equivalent control law U_{eq} which keeps the state of the system on the sliding surface. The equivalent control law is obtained by the following equation:

$$\dot{s}\,|_{U=U_{eq}} = 0\,. \tag{15}$$

Assuming all uncertainty factors are zero, then we have

$$C_1e_2 + C_2e_3 + \hat{f} + \hat{g}U_{eq} + \hat{f}_L - \dddot{x}_d = 0 \tag{16}$$

Solving Equation (16) yields

$$U_{eq} = -\hat{g}^{-1}(C_1e_2 + C_2e_3 + \hat{f} + \hat{f}_L - \dddot{x}_d) \tag{17}$$

3.2. Hitting Control Law Design

A Lyapunov function candidate is chosen as follows:

$$V = \frac{1}{2}s^2(X,t) \tag{18}$$

It is shown that if there exists a positive constant η, such that

$$\dot{V} = \frac{1}{2}\frac{d}{dt}(s^2(X,t)) \leq -\eta|s| < 0 \tag{19}$$

then the state trajectories hit the sliding surface s. In order

to satisfy the hitting condition of Equation (19) in the presence of uncertainties, the hitting control law is chosen as:

$$U_n = -\hat{g}^{-1}(K\,\mathrm{sgn}(s)), (K>0)\,, \tag{20}$$

where

$$\mathrm{sgn}(s) = \begin{cases} 1 & \text{if } s>0 \\ 0 & \text{if } s=0 \\ -1 & \text{if } s<0 \end{cases} \tag{21}$$

Equation (19) will be

$$\dot{V} = s\dot{s} = s(C_1e_2 + C_2e_3 + f + gU + f_L - \ddot{x}_d) \le -\eta|s| < 0\,. \tag{22}$$

Equation (22) can be represented as

$$[C_1e_2 + C_2e_3 + f + f_L - \ddot{x}_d]\mathrm{sgn}(s) + gU\,\mathrm{sgn}(s) \le -\eta \tag{23}$$

Substituting Equations (14), (17) and (20) into (23) yields

$$\begin{aligned}&[C_1e_2 + C_2e_3 + f + f_L - \ddot{x}_d]\mathrm{sgn}(s) - \frac{g}{\hat{g}} \\ &(C_1e_2 + C_2e_3 + \hat{f} + \hat{f}_L - \ddot{x}_d)\mathrm{sgn}(s) - \frac{g}{\hat{g}}K \le -\eta\end{aligned} \tag{24}$$

The optimal value of K will be

$$\begin{aligned}K \ge \frac{1}{g}\Big[&\hat{g}(\tilde{f} + \tilde{f}_L + \eta\,\mathrm{sgn}(s)) - \\ &\tilde{g}(C_1e_2 + C_2e_3 + \hat{f} + \hat{f}_L - \ddot{x}_d)\Big]\mathrm{sgn}(s)\end{aligned} \tag{25}$$

To alleviate the chattering phenomenon, the quasi-linear mode controller (Slotine and Li, 1991), which replaces the discontinuous control laws of Equation (20), is adopted. The U_n in Equation (20) is replaced by

$$U_n = -\hat{g}^{-1}\left(K\,\mathrm{sat}\left(\frac{s}{\varepsilon}\right)\right) \tag{26}$$

where $\varepsilon>0$ is the width of boundary, and the function of $\mathrm{sat}(s/\varepsilon)$ is defined as

$$sat\left(\frac{s}{\varepsilon}\right) = \begin{cases} 1 & \text{if } s>\varepsilon, \\ \dfrac{s}{\varepsilon} & \text{if } -\varepsilon \le s \le \varepsilon \\ -1 & \text{if } s<-\varepsilon. \end{cases} \tag{27}$$

This leads to tracking within a guaranteed precision ε, while allowing the alleviation of the chattering phenomenon.

4. DESIGN OF THE EFSMC

In the general sliding mode control, the switching feedback gain K in Equation (26) is a constant, which can influence the performance of the sliding mode controller. Figure 4 shows the effects of the switching control gain K on the control performance (Abdelhameed, 2005). If K is large, the system states reach the sliding surface quickly, but a considerable amount of overshoot is noticeable. In addition, the chattering would occur as depicted in curve "A". If K is small, it takes a longer time to reach the sliding surface. The sliding line may be shown in curve "B" and the chattering phenomenon is weakened. The curve "C" represents the desired curve to be attained. Therefore, a fuzzy logic adaptation system (FLAS) is adopted here, in which a fuzzy inference mechanism is used to estimate the switching feedback gain K. The sliding surfaces s and $\dot{s}$ are considered as the inputs of the fuzzy adaptation system. Compared with the conventional estimator, the fuzzy inference mechanism uses prior expert knowledge to accomplish the control object more efficiently.

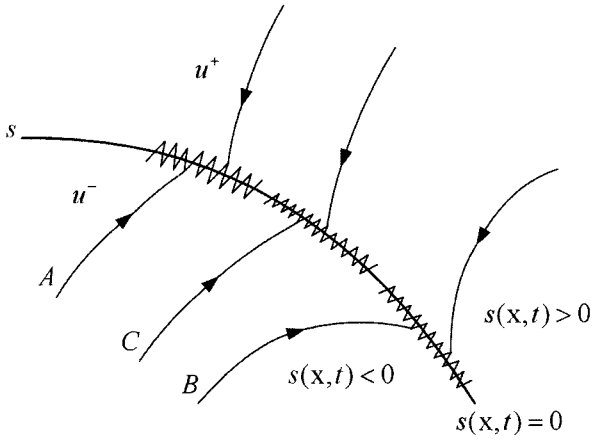

Figure 4. Effects of the switching control gain K on the control performance.

4.1. Region-Wise Linear Fuzzy Logic Adaptation System (RWLFLAS)

One key aspect involved in the design of the FLAS is the complexity of the fuzzy logic controllers, which increases as the number of fuzzy if-then rules increases. The number of rules increases exponentially as the number of input variables of fuzzy controller increases. If Γ is the number of fuzzy sets for s and $\dot{s}$, the number of the complete rule bases is equal to $\Gamma_s \times \Gamma_{\dot{s}}$. In order to reduce the number of fuzzy control rules in the FLAS, the region-wise linear technique (Fung and Shaw, 2000) is adopted. Therefore, the EFSMC is proposed here, in which a region-wise linear fuzzy inference mechanism is used to decrease the complexity of the FLAS.

Figure 5 shows a block diagram of the proposed enhanced fuzzy logic adaptive sliding mode controller. The RWLFLAS is proposed to adapt the switching gain K in order to achieve desired tracking while minimizing the reaching time, chattering of the control action and the

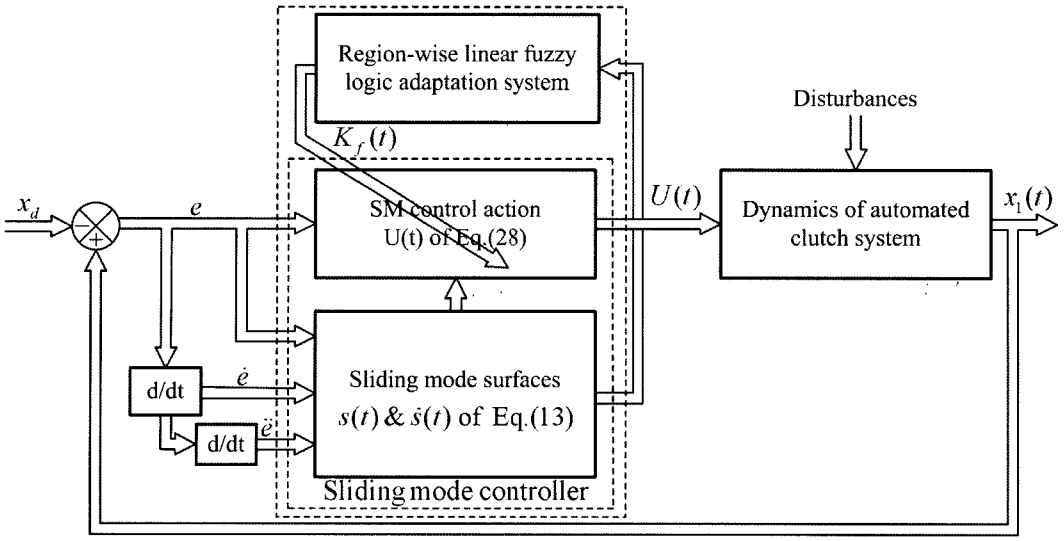

Figure 5. Block diagram of the enhanced fuzzy sliding mode controller.

computational burden of ECU, all without causing overshoot or instability. The RWLFLAS balances the chattering and the error in the system and tunes the switching feedback control gain K in such a way to achieve best tracking. Replacing K by K_f in Equation (26), the following control law can be obtained

$$U(t)=U_{eq}-\hat{g}^{-1}\left(K_f \text{sat}\left(\frac{s}{\varepsilon}\right)\right), \tag{28}$$

where K_f is adjusted by the RWLFLAS.

4.2. Design of the RWLFLAS

The RWLFLAS consists of three modules as depicted in Figure 6: fuzzification, inference engine and defuzzification. The main goal for the RWLFLAS is to obtain a gain change Δk_f so that the switching feedback control gain K_f varies with the automated clutch configuration. Since the output K_f is in its corresponding universe of discourse, the output change Δk_f of RWLFLAS could then be transferred by multiplying a scaling factor GK (Fung *et al.*, 1999). And ΔK_f can be given by

$$\Delta K_f = GK * \Delta k_f \tag{29}$$

The actual output is defined as

$$K_f(n)=K_f(n-1)+\Delta K_f \tag{30}$$

where n is the number of iterations.

The signals s and $\dot{s}$ should be transferred to their corresponding universes of discourses by multiplying scaling factors GS and GDS respectively as

$$S = s*GS,\ \dot{S}=\dot{s}*GDS \tag{31}$$

To achieve the control objective, a scaling factor tuner (SFT) is introduced to tune the scaling factor GK The output of the SFT is determined by the following strategies: (1) when the state of the represented point is near or approaching the sliding surface, a small control signal is required. Hence, we reduce the value of scaling

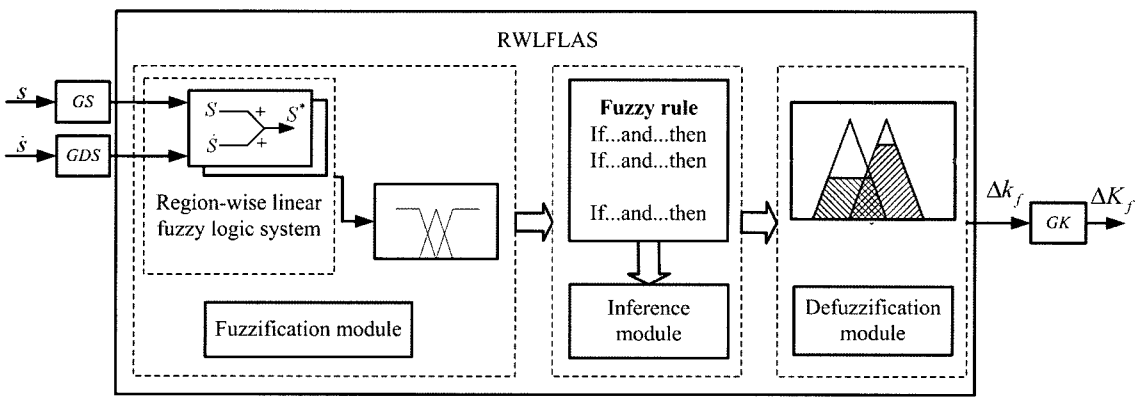

Figure 6. Structure of the RWLFLAS.

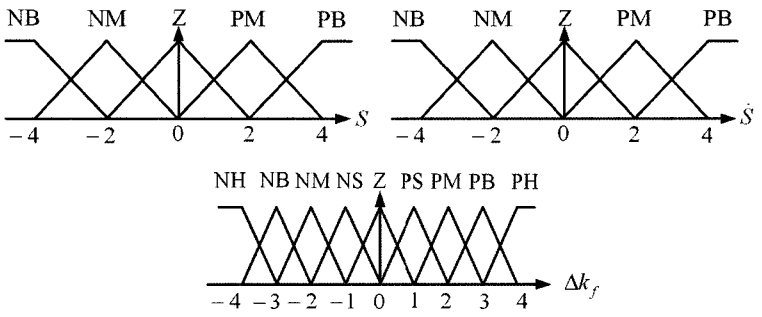

Figure 7. Membership functions of S, $\dot{S}$ and Δk_f.

factor; (2) when the state of the represented point is far from the sliding surface, the value of scaling factor must be enlarged so as to make the state approach toward the sliding surface faster. The SFT is given by

$$\begin{cases} \text{IF} \quad |s| \geq s_c, & \text{THEN} \quad GK = a_s * e_1^{k_{s1}} \\ \text{IF} \quad |s| < s_c, & \text{THEN} \quad GK = b_s * e_1^{k_{s2}} \end{cases} \tag{32}$$

where a_s, b_s, k_{s1} and k_{s2} are the constants, and e_1 is the error of the actual and desired trajectories. s_c is a positive switch constant that is determined according to the sliding surface.

In order to reduce the number of fuzzy control rules in the FLAS, the inputs S and S are linearized using the region-wise linear technique. The conventional FLAS membership functions of inputs S, $\dot{S}$ and output Δk_f are defined in Figure 7. There is no universal method to determine their values. Therefore, simple trial and error is used in practice and the discourses are all assigned to be [-4, 4]. The significance of the universe of discourse lies in the fact that the input variables belonging to each universe of discourse are mapped from measured values with corresponding scaling factors, respectively. The fuzzy logic system rules are shown in Table 1.

IF S is PB *and* $\dot{S}$ *is* PB, *THEN* Δk_f *is* NH. This control rule states that if S and $\dot{S}$ have large positive values, which is equivalent to $s\dot{s}$ being largely positive, then a large negative change of the control input is required to decrease $s\dot{s}$ quickly.

IF S is PB *and* $\dot{S}$ *is* NB *THEN* Δk_f *is* Z *or IF v is* NB *and* $\dot{S}$ *is* PB *THEN* Δk_f *is* Z

This control rule implies a situation when $s\dot{s}$ is largely negative, which is the desired situation, and there is no need to change the control input.

·*IF S is* NB *and* $\dot{S}$ *is* NB *THEN* Δk_f *is* PH

This control rule states that if S and $\dot{S}$ have large negative values, which is equivalent to that $s\dot{s}$ being largely positive, then, a large positive change of the control input is required to decrease $s\dot{s}$ quickly.

From Table 1, the fuzzy control rule bases for the fuzzy logic controller are symmetric, and the output variable of the controller depends on the negative weight sum of two input variables (Yu *et al.*, 1998). Therefore, we defined

$$S^* = S + \dot{S} \tag{33}$$

Let the input and output fuzzy variables of the RWLFLAS have nine linguist labels that are denoted by PH, PB, PM, PS, Z, NS, NM, NB and NH. The relationships between S, $\dot{S}$ and S^* are list in Table 2. The rule bases for the RWLFLAS are depicted in Table 3. Membership functions of S^* and Δk_f are shown in Figure 8. In order to implement this fuzzy controller in the ECU

Table 1. Linguistic rules based on the FLAS.

	Δk_f	$\dot{S}$				
		NB	NM	Z	PM	PB
S	NB	PH	PB	PM	PS	Z
	NM	PB	PM	PS	Z	NS
	Z	PM	PS	Z	NS	NM
	PM	PS	Z	NS	NM	NB
	PB	Z	NS	NM	NB	NH

The linguistic control rules are defined as
N: Negative, Z: Zero, P: Positive, NH: Negative Huge, NB: Negative Big, NM: Negative Medium, NS: Negative Small, PS: Positive Small, PM: Positive Medium, PB: Positive Big, PH: Positive Huge
For the purpose of illustration, a few control rules in Table 1 are described below:
IF S is PB *and* $\dot{S}$ *is* PB, *THEN* Δk_f *is* NH

Table 2. Relationships between S^*, S and $\dot{S}$.

	S^*	$\dot{S}$				
		NB	NM	Z	PM	PB
S	NB	NH	NB	NM	NS	Z
	NM	NB	NM	NS	Z	PS
	Z	NM	NS	Z	PS	PM
	PM	NS	Z	PS	PM	PB
	PB	Z	PS	PM	PB	PH

Table 3. Rule base for the Region-wise linear fuzzy logic system.

S^*	PH	PB	PM	PS	Z	NS	NM	NB	NH
Δk_f	NH	NB	NM	NS	Z	PS	PM	PB	PH

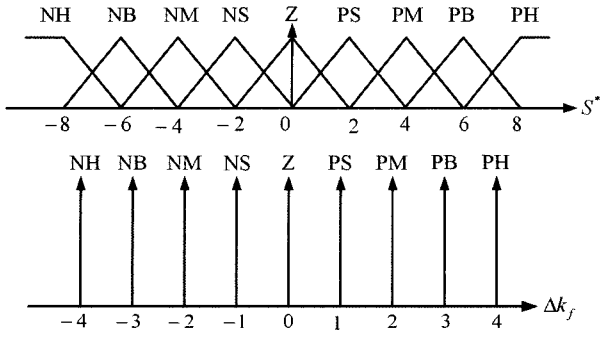

Figure 8. Membership functions of S^* and Δk_f.

in real-time, the fuzzy inference mechanism will be simplified to build a decision look-up table by the mapping process.

The input for the defuzzification process is a fuzzy set (the aggregate out fuzzy set) and the output is a single crisp number. This output represents the output of the RWLFLAS. In this paper, a center average defuzzification, a Mamdani implication in the rule base and a product inference engine are used in designed defuzzification module. The output of the RWLFLAS can be written as:

$$\Delta k_f = \frac{\sum_{i=1}^{r} \alpha_i \prod_{j=1}^{h} \mu_{ij}(S^*)}{\sum_{i=1}^{r} \prod_{j=1}^{h} \mu_{ij}(S^*)} \tag{34}$$

where r is the number of rules, h is the number of inputs, $\alpha = [\alpha_1, \ldots, \alpha_i, \ldots, \alpha_r]^T$ is the vector of the centers of the membership functions of Δk_f.

4.3. Stability Analysis for the EFSMC

In this section, the EFSMC system is checked for stability and robustness with regard to parameter fluctuations of the original system (8), in which the switching feedback gain can be estimated by adopting the RWLFLAS. However, the switching gain is a constant for the CSMC, and the reachable condition has to be met as follows

$$K = \max\left\{\frac{1}{g}\left[\hat{g}(\tilde{f} + \tilde{f}_L + \eta \operatorname{sgn}(s)) - \tilde{g}(C_1 e_2 + C_2 e_3 + \hat{f} + \hat{f}_L - \ddot{x}_d)\right]\operatorname{sgn}(s)\right\} \tag{35}$$

where ζ is a positive constant.

For the EFSMC, the switching gain can be adjusted according to the input of RWLFLAS S^*; therefore, the Lyapunov function $\dot{V}$ has to be met, substitute equation (13), (28) into (19)

$$\begin{aligned} \dot{V} = s\dot{s} &= s(C_1 e_2 + C_2 e_3 + \dddot{x} - \dddot{x}_d) \\ &= s\left[\tilde{f} + \tilde{f}_L - \frac{\tilde{g}}{\hat{g}}(C_1 e_2 + C_2 e_3 + \hat{f} + \hat{f}_L - \dddot{x}_d) - \frac{\tilde{g}}{\hat{g}} K_f \operatorname{sat}\left(\frac{s}{\varepsilon}\right)\right] \le -\eta|s| \end{aligned} \tag{36}$$

then, the output of RWLFLAS Δk_f

$$\Delta k_f \ge \frac{\operatorname{sat}(s/\varepsilon)}{GU}\left\{\frac{\hat{g}}{g}\left[\tilde{f} + \tilde{f}_L - \frac{\tilde{g}}{\hat{g}}(C_1 e_2 + C_2 e_3 + \hat{f} + \hat{f}_L - \dddot{x}_d)\right] \operatorname{sgn}(s) + \eta - K_f(n-1)\right\} \tag{37}$$

Δk_f can satisfy the condition (36) by adjusting the parameters of GU, which satisfy the Lyapunov function $\dot{V} \le s\dot{s} < 0$.

5. NUMERICAL SIMULATION

To illustrate the effectiveness and robustness of the proposed controller, the numerical simulation of launch control has been carried out on the automated clutch. In order to compare the performance of the proposed controller with that of the CSMC, the system parameters, the coefficient of the hyperplane and external disturbances are chosen to be the same. The vehicle launch of automated clutch is driven according to the following desired trajectory, which is obtained from the experiment data (Liu and Zhang, 2002).

$$x_d = 8\times10^{-3} - 1.633\times10^{-2}\, t^2, \quad (x_d \ge 0) \tag{38}$$

With a nonlinear dynamic system for the automated clutch, the performance measures such as reaching time t_r are recommended (Lin *et al.*, 2001). Furthermore, the computational time of each iterative step for EFSMC, FSMC and CSMC is introduced during the simulation.

According to the Hurwitz polynomial, suppose the eigenroot of the sliding mode is [–979.6, –20.4], then $C_1 = 2\times10^4$, $C_2 = 1\times10^3$. In addition, the gains of the conventional sliding mode control law are obtained by using $\varepsilon = 0.01$ and $K = 5\times10^4$, and the parameters of SFT are given by $s_c = 10$, $a_s = 2.0\times10^4$, $b_s = 10$, $k_{s1} = 0.9$ and $k_{s2} = 0.9$.

The parameters of the automated clutch are chosen in numerical simulations as follows:

$p = 4$, $R = 0.21\Omega$, $L\text{-}M = 1.49\times10^{-3}$ H, $\lambda_m = 0.105$Vs/rad, $J_e = 1.913\times10^{-4}$ kg.m^2, $B_m = 0.1$Nm/s, $K_A = 12.5$, $G_I = 10$, $V_{DC} = 12$V, $A_d = 6.0$V, $k_d = 4.552\times10^{-5}$, $k_T = 0.02$, cm$= 0.1$N/s.

The simulation time is 0.8s. The sampling time step size for simulation is 0.4 ms. The objective is to control the clutch to move from the initial position to the end. Hence, the vehicle launch can be analyzed in this investi-

gation adopting the CSMC and EFSMC methods respectively.

Considering the worst working condition of the automated clutch, many uncertain states will occur during the running period of vehicle when the automated clutch of the AMT vehicle works in the worst condition. For example, the clutch is being detached and the deduction of ECU is obtained by judging the input signals, which requires the clutch to engage immediately, or the initial position of the clutch is changed due to installation error and there is a longer time wear and tear during the running period. To improve the safety of the vehicle and to reflect driver's intention quickly, it is desirable for the control system to have the capacity for fast recoveries from the abnormal instances. Therefore, in order to reflect the actual work state of automated clutch, the external disturbance force is chosen as f_E=−50N~50N; the parameters of automated clutch, a_2, a_3 and b can fluctuate in ±10% randomly. The initial position of clutch is assumed to be 9 mm.

The dynamic responses obtained by employing the CSMC and EFSMC to the automated clutch have been shown in Figures 9 and 10, which shows the tracking performance, tracking errors, controlling actions and sliding surfaces, respectively. Figures 9(c) and 10(c) show that the control input current i_q^* has one jerk in the inflexion of the tracking trajectory at the exact moment 0.7s.

A faster tracking response can be observed by employing the proposed EFSMC. The sliding surface s can be decreased rapidly as shown in Figure 10(d). During the sliding phases, the actual trajectory response of EFSMC approaches the desired trajectory $x_d(t)$. The chattering phenomenon of the control response i_q^* can be observed both in Figure 9(c) and Figure 10(c), and a noticeable increase of the control action i_q^* in Figure 10 (c) is observed during the reaching phase. A faster tracking response is observed by employing the proposed EFSMC and the reaching times t_r for CSMC and EFSMC are 0.18s and 0.06s, respectively. The reaching time is decreased by 66.7%. After the reaching time t_r, the actual trajectory response $x_1(t)$ is almost identical to the desired command $x_d(t)$. However, the computational time of each iterative step for FSMC, EFSMC and CSMC are 0.547 ms, 0.379 ms and 0.215 ms, respectively (including the model of automated clutch) during the process of simulation. Compared with the FSMC, the computational time of each iterative step for EFSMC has been shortened by 30.7%, which can satisfy the real-time requirement of the automated clutch system of AMT.

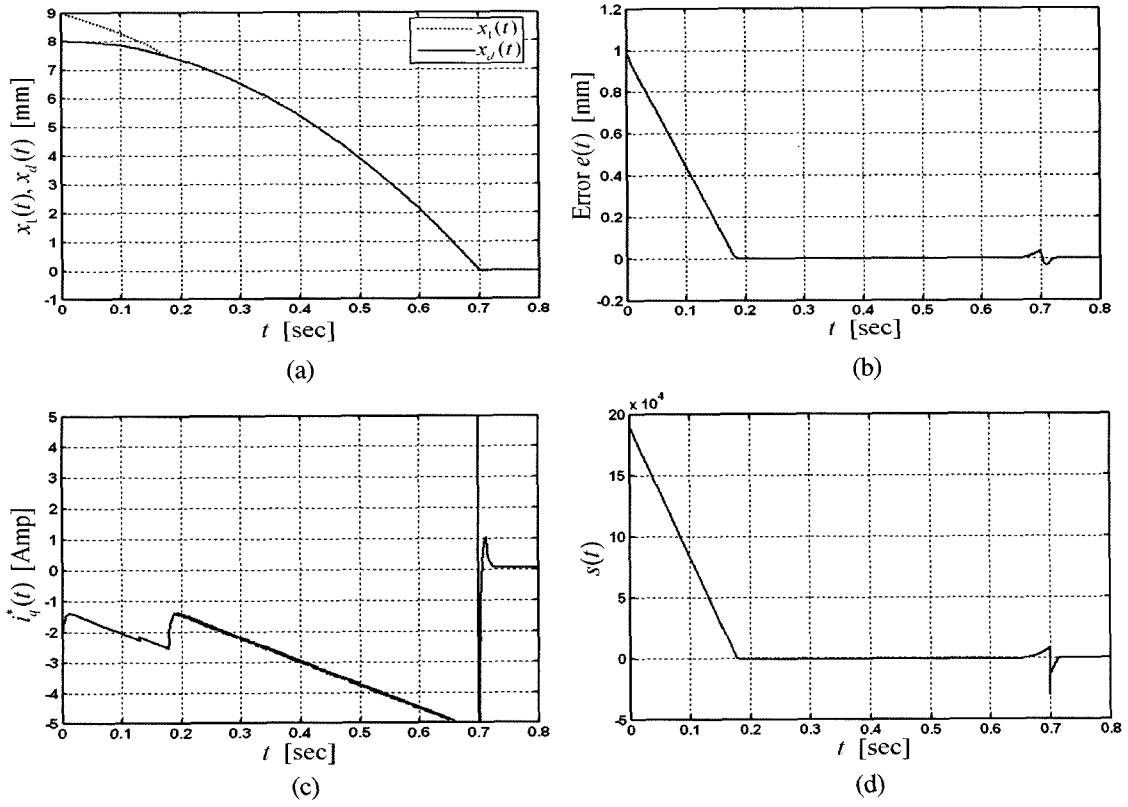

Figure 9. Response trajectories of CSMC (a) clutch position trajectory $x_1(f)$ and $x_d(t)$ (b) error $e(t)$ (c) control input $i_q^*(t)$ (d) sliding mode surface $s(t)$.

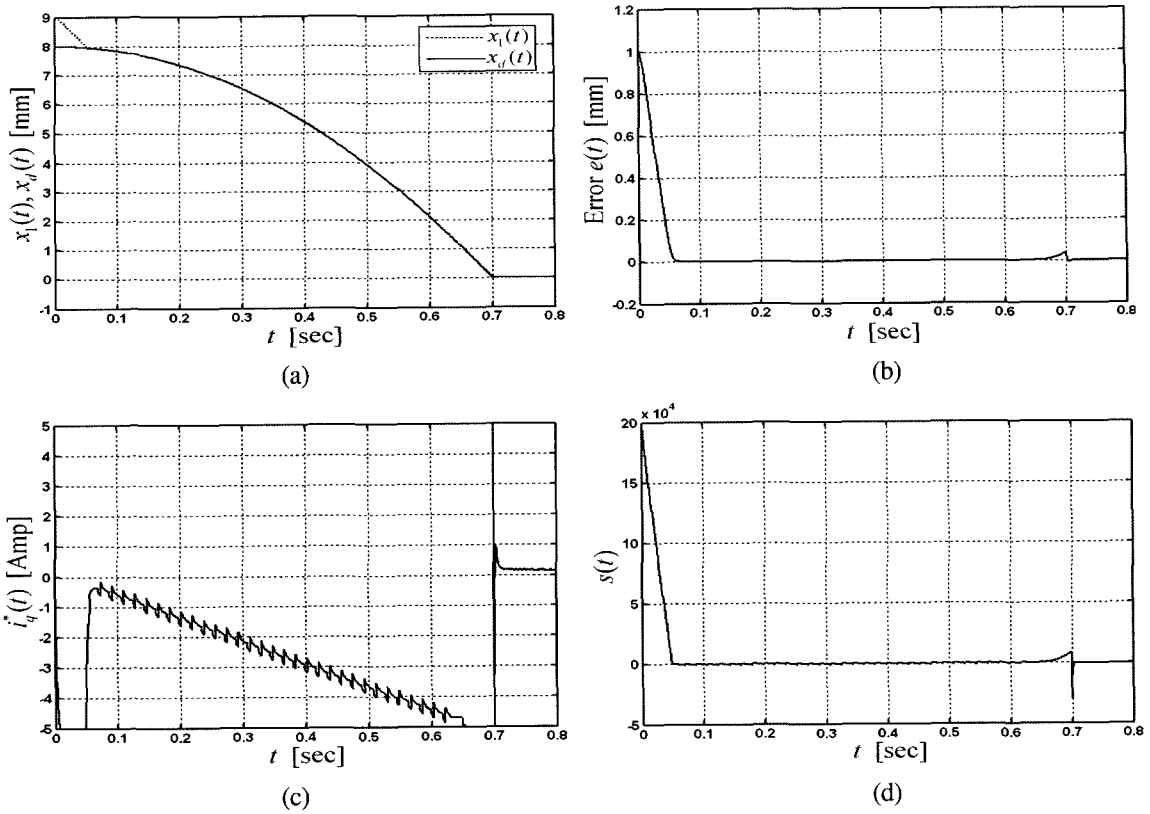

Figure 10. Response trajectories of EFSMC (a) clutch position trajectory $x_1(f)$ and $x_d(t)$ (b) error $e(t)$ (c) control input $i_q^*(t)$ (d) sliding mode surface $s(t)$.

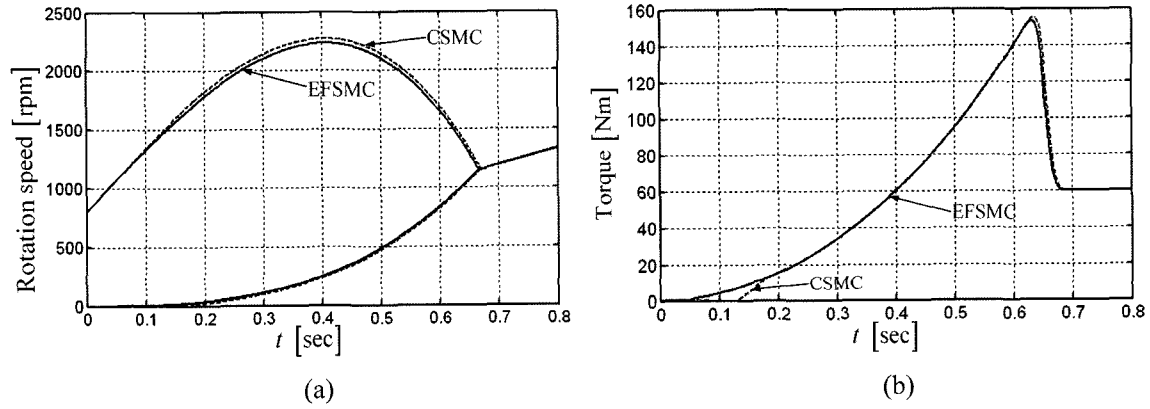

Figure 11. Outputs of speed and torque adopting EFSMC and CSMC, respectively.

The output rotate speed and torque of the automated clutch adopting EFSMC and CSMC are shown in Figure 11. The rotate speed of the automated clutch can be increased more flatly by using the proposed EFSMC than by using CSMC as shown in Figure 11(a), which can improve the passenger comfort and lessen friction loss. Correspondingly, the output torque of the automated clutch system transmitted from the engine to the clutch is also more blandly than by adopting the EFSMC during the launch process. Therefore, the AMT vehicle can be rapidly launched which reflects the intention of driver and decrease the impact by adopting the EFSMC.

6. CONCLUSIONS

This paper has proposed an enhanced sliding mode cont-

roller and applied the controller to the position control of the automated clutch for AMT vehicle launch using a brushless DC motor drive. A complete mathematical model of the automated clutch with brushless DC motor driving was developed. The region-wise linear technology was used to decrease the fuzzy rules of FLAS; the speed of fuzzy inference was improved and the computational time was reduced. The simulation results demonstrate the effectiveness and robustness of the proposed controller.

REFERENCES

Abdelhameed, M. M. (2005). Enhancement of sliding mode controller by fuzzy logic with application to robotic manipulators. *MECHATRONICS*, **15**, 439–458.

Chen, J and Tang, P. C. (1999). A sliding mode current control scheme for PWM brushless DC motor drives. *IEEE Trans. Power Electronics* **14**, **3**, 541–551.

Chen, L., Zhang, J. W. and Xi, G. (2000). Feedback linearization control for electronically controllable clutch of vehicle. *SAE Paper No.* 2000-01-1638.

David, J. and Natarajan, N. (2005). Design of an optimal clutch controller for commercial trucks. *Proc. 2005 American Control Conf.*, Portland, OR, USA, 1599–1606 (AACC, Dayton).

Faiz, J., Azizian, M. R. and Aboulghasemian-Azami, M. (1996). Simulation and analysis of brushless DC motor drives using hysteresis, ramp comparison and predictive current control techniques. *Simulation Practice and Theory*, **3**, 347–363.

Fung, R. F., Chen, K. W. and Yen, J. Y. (1999). Fuzzy sliding mode controlled slider-crank mechanism using a PM synchronous servo motor drive. *Int. J. Mechanical Sciences*, **41**, 337–355.

Fung, R. F. and Shaw, C. C. (2000). Region-wise linear fuzzy sliding mode control of the motor-mechanism systems. *J. Sound and Vibration* **234**, **3**, 471–489.

Gaillard, C. L. and Singh, R. (2000). Dynamic analysis of automotive clutch dampers. *Applied Acoustics*, **60**, 399–424.

Garofalo, F. and Glielmo, L. (2001). Smooth engagement for automotive dry clutch. *Proc. 40th IEEE Conf. Decision and Control*, Orlando, Florida USA, 529–534 (IEEE, New York).

Glielmo, L., Iannelli, L., Vacca, V. and Vasca, F. (2006). Gearshift control for automated manual transmissions. *IEEE/ASME Trans. Mechatronics* **11**, **1**, 17–26.

Glielmo, L. and Vasca, F. (2000). Engagement control for automotive dry clutch. *Proc. 2000 American Control Conference*, Chicago, Illinois, 1016–1017 (AACC, Dayton).

Ha, Q. P., Rye, D. C. and Durrant-Whyte, H. F. (1999). Fuzzy moving sliding mode control with application to robotic manipulators. *Automatic*, **35**, 607–616.

Hahn, J. O. and Lee, K. I. (2002). Nonlinear robust control of torque converter clutch slip system for passenger vehicles using advanced torque estimation algorithms. *Vehicle System Dynamics* **37**, **3**, 175–192.

Hayashi, Y., Shimizu, Y. and Nakanura, S. Dote, Y. Takayama, A. Hirako, A. (1993). Neuro fuzzy optimal transmission control for automobile with variable loads. *Proc. IECON' 93 Int. Conf. Industrial Electronics, Control and Instrumentation*, **1**, 430–434 (IEEE, New York).

Hibino, R., Osawa, M. and Yamada, M. (1996). H^{∞} Control design for torque-converter-clutch slip system. *Proc. 35th Conf. Decision and Control*, Kobe, Japan, 1797–1802 (IEEE, New York).

Horn, J., Bamberger, J. and Michau, P. (2003). Flatness-based clutch control for automated manual transmissions. *Control Engineering Practice*, **11**, 1353–1359.

Kaynak, O, Erbatur, K and Ertugrul, M. (2001). The fusion of computationally intelligent methodologies and sliding mode control-A survey. *IEEE Trans. IE.* **48**, **1**, 4–17.

Lee, J. H. and Youn, M. J. (2004). A new improved continuous variable structure controller for accurately prescribed tracking control of BLDD servo motors. *Automatica*, **40**, 2069–2074.

Lin, J. M., Lin, M. C. and Wang, H. P. (2001). LEQG/LTR controller design with extended Kalman filter for sensorless brushless DC driver. *Comput. Methods Appl. Mech. Engrg.*, **190**, 5481–5494.

Liu, F., Li, Y. and Zhang, J. W. (2002). Robust control for automated clutch of AMT vehicle. *SAE Paper No.* 2002-01-0933.

Montanari, M. and Ronchi, F. (2004). Control and performance evaluation of a clutch servo system with hydraulic actuation. *Control Engineering Practice*, **12**, 1369–1379.

Phakamach, P., Tiacharoen, S. and Akkaraphong, C. (2002). Position control of a brushless DC servomotor using a sliding mode model following control (SMFC) system. *IEEE ICIT'02*, Bangkok, THAILAND, 566–571. (IEEE, New York)

Shen, S. W. and Wu, C. Q. (1999). 15An expert fuzzy control of automatic mechanical transmission clutch. *SAE Paper No.* 1999-01-2814.

Slotine, J. and Li, W. P. (1991). *Applied Nonlinear Control.* Prentice-Hall. Englewood Cliffs, New Jersey.

Slicker, J. M. and Loh, R. N. K. (1996). Design of robust vehicle launch control system. *IEEE Trans. Control Systems Technology* **4**, **4**, 326–335.

Tanaka, H. and Wada, H. (1995). Fuzzy control of clutch engagement for automated manual transmission. *Vehicle System Dynamics*, **24**, 365–376.

Transmission of AUTO. (2005). http://auto.sina.com.cn/

news/2005-02-01/111998098.shtml

Wu, H. X., Cheng, S. K. and Cui, S. M. (2005). A controller of brushless DC motor for electric vehicle. *IEEE Trans. Magnetics*, **41**, **1**, 509–513.

Yu, F. M., Chung, H. Y. and Chen, S. Y. (2003). Fuzzy sliding mode controller design for uncertain time-delayed systems with nonlinear input. *Fuzzy Sets and Systems*, **140**, 359–374.

Yu, X. H., Man, Z. H. and Wu, B. L. (1998). Design of fuzzy sliding-mode control systems. *Fuzzy Sets and Systems*, **95**, 295–306.

Zanasi, R. and Visconti, A. (2001). Dynamic modeling and control of a car transmission system. *Proc. 2001 IEEE/ASME Int. Conf. Advanced Intelligent Mechatronics*, Como, Italy, 416–421 (IEEE/ASME, New York).

Zhang, J., Chen, L. and Xi, G. (2002). System dynamic modeling and adaptive optimal control for automatic clutch engagement of vehicles. *Proc. Instn. Mech. Engrs., Part D: Automobile Engineering*, **216**, 983–991.